Bulk rock composition : a key to identifying invisible prograde reactions in zoned garnet

Autor(en):   **Hetherington, Callum J. / Le Bayon, Ronan**

Bulk rock composition: a key to identifying invisible prograde reactions in zoned garnet

Callum J. Hetherington[1*] and *Ronan Le Bayon*[2**]

Abstract

Chemical zonation of prograde metamorphic minerals is commonly attributed to net transfer reactions, intra-crystalline diffusion or the growth of compositionally differing zones of the same phase during consecutive geological events. Evidence for such events or processes is commonly recorded in mineral relics and/or inclusions, or through the interpretation of geochronological data.

Complex chemical zonation has been recorded in garnet grains from garnet–biotite–muscovite gneiss from the Berisal Complex, Simplon Region, Switzerland. None of the features (e.g. relic inclusions) used to interpret such zoning via petrography are observed or applicable; therefore, the reactions occuring on the prograde P–T path and its shape and trajectory cannot be defined. In the absence of features necessary to permit a classical investigation of equilibrium-disequilibrium phases and their role in the growth of the garnets, an approach based on the bulk rock composition of the rock has been investigated.

For a given bulk rock chemistry, equilibrium phase diagrams are constructed over a specified P–T range using DOMINO software. Important minerals are identified and their isopleths calculated to model the variation in composition of each phase in response to variations in pressure and temperature. The modelled chemical changes are compared with the observed chemical zonations and the Alpine metamorphic history of the gneiss and its garnet grains is reconstructed.

The modelling of the prograde mineral reactions using a rock's bulk rock composition, combined with observed chemical zonations in metamorphic minerals, is a valuable method for constraining the prograde P–T path when standard methods are inapplicable.

Keywords: Zoned garnet, prograde metamorphic reactions, P-T-X conditions, bulk rock composition, Berisal Complex.

1. Introduction

1.1. Chemical Zoning in Metamorphic Minerals

Chemical zoning in metamorphic minerals can be studied to aid understanding of the evolution of their host rock. The development of chemical zoning in primary metamorphic minerals, such as garnet, is strongly influenced by three mechanisms. At lower temperatures, where intra-crystalline element diffusion rates are low, chemical zones in a mineral result from net transfer reactions. Net transfer reactions exert a first order control over the local chemical environment in which a mineral is growing (Chernoff and Carlson, 1997), for the breakdown and formation of metamorphic phases enriches or depletes respectively, the effective bulk composition of the equilibration volume (defined as the volume of rock, which at a given P and T reacts to be in chemical equilibrium; Stuewe, 1997).

At higher temperatures, in addition to the role of net transfer reactions, intra-granular diffusion processes are increasingly important (O'Brien, 1999). Such diffusion, occurring in response to compositional gradients within a crystal or between phases, preserves a record of the rock's attempt to adapt to changing conditions. This process is effectively restricted to high-temperature (granulite facies) metamorphic conditions, and evidence has been documented in garnet from such environments (O'Brien, 1999; O'Brien and Vrana, 1997).

Chemical zonation in metamorphic minerals, particularly garnet, may also result after incomplete recrystallisation of a mineral core from a previous metamorphic cycle. The residual core may act as a nucleus for new mineral growth in a later metamorphic event (Rollinson, 2003). Thus, mineral relics that survive from one metamorphic event to the next may be overgrown by a second

[1] Natural History Museum, University of Oslo, PO Box 1172 Blindern, NO-0318 Oslo, Norway.
[*] Present address: Department of Geosciences, University of Massachusetts, 611 North Pleasant Street, Amherst, MA 01003-9297, USA. *Corresponding author* <callum@geo.umass.edu>
[2] Department of Earth Sciences, University of Basel, Bernoullistrasse 30, CH-4056 Basel, Switzerland.
[**] Present address: Institut für Geowissenschaften, Technische Universität Darmstadt, Schnittspahnstrasse 9, 64287 Darmstadt, Germany.

generation of the same mineral with a different chemical composition.

Chemical zoning in minerals has more commonly been used in recent years to elucidate the metamorphic history of samples. Where suitable mineral relics or inclusions exist, it is possible to reconstruct the succession of metamorphic mineral assemblages that existed earlier in the rock's history and thereby reconstruct a P–T path (Escuder Vituete et al., 2000; Simon et al., 1997; Zeh, 2001a, 2001b; Zeh and Holness, 2003). In the case of multiple phases of growth it is sometimes possible to date the different zones by step-wise leaching of a suitable isotope system (Kreissig et al., 2001).

1.2. Zoned garnet grains from the Berisal Complex

Zoned garnet grains occur in a garnet-biotite-muscovite paragneiss that outcrops in the pre-Mesozoic crystalline basement rocks of the Berisal Complex, Simplon Region, Switzerland. This Complex, structurally the uppermost unit of the western Lepontine dome, consists of several polymetamorphosed crystalline basement litho-logies enveloped in metasediments which experienced solely Alpine metamorphism.

The garnet–biotite–muscovite gneiss has been interpreted as a paragneiss (Hetherington, 2001; Stille, 1980) that was intruded by a 1 Ga suite of

Table 1   Representative electron-microprobe analysis from each zone of a garnet grain.

	Garnet				
Zone	**1**	**2**	**3**	**3**	**4**
Analysis	**a**	**b**	**c**	**d**	**e**
SiO_2	36.68	37.35	37.68	37.46	37.38
TiO_2	0.22	0.15	<0.15	0.10	<0.15
Al_2O_3	20.03	20.57	20.82	20.63	20.63
Cr_2O_3	<0.15	0.03	0.08	0.05	0.11
FeO	34.53	28.41	33.52	36.81	36.06
MnO	7.23	5.47	1.72	0.47	0.09
MgO	1.64	1.07	2.17	3.10	3.18
CaO	0.71	7.95	4.92	2.21	3.68
Total	101.0	101.0	100.9	100.8	101.1
Si	2.99	2.99	3.01	3.00	2.99
Ti	0.01	0.01	0.00	0.01	0.00
Al	1.92	1.94	1.96	1.95	1.94
Cr	0.00	0.01	0.01	0.00	0.01
Fe	2.35	1.90	2.24	2.47	2.41
Mn	0.50	0.37	0.04	0.03	0.01
Mg	0.20	0.13	0.26	0.19	0.38
Ca	0.06	0.68	0.42	0.19	0.32
Cations	8.04	8.03	8.03	8.02	8.05
X_{Prp}	**0.04**	**0.04**	**0.09**	**0.12**	**0.12**
X_{Alm}	**0.76**	**0.62**	**0.74**	**0.81**	**0.77**
X_{Grs}	**0.02**	**0.22**	**0.14**	**0.06**	**0.10**
X_{Sps}	**0.16**	**0.12**	**0.04**	**0.01**	**0.00**

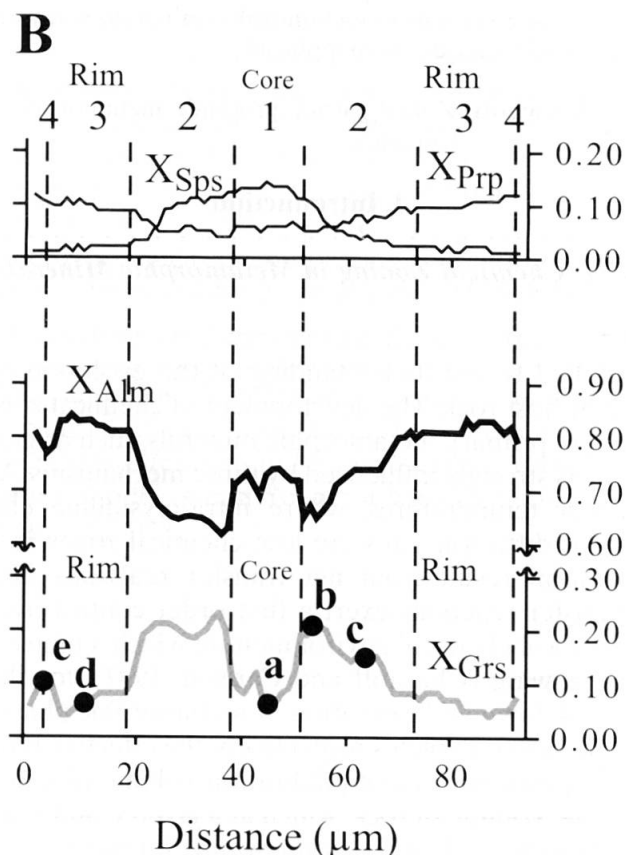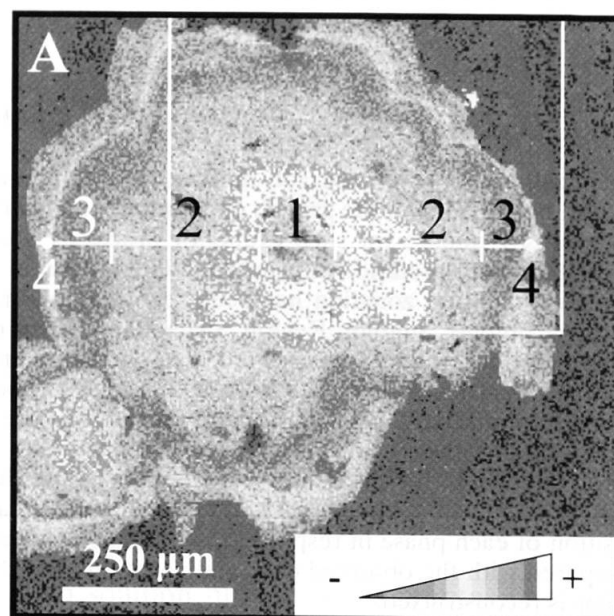*Notes:* Zone numbers and analysis points refer to those labelled in Fig. 1B.

Fig. 1   (A) X-ray map for Ca in a zoned garnet grain from garnet–biotite–muscovite gneiss. (B) Line-scan profiles across the centre of the zoned garnet. For explanation of each numbered garnet composition zone see text. Letters a–e refer to individual chemical analyses (Table 1).

tholeiitic-dacites, which define the minimum age of sediment deposition (Stille and Tatsumoto, 1985). The gneiss consists of bands that are, generally, chemically and mineralogically homogenous (Hetherington, 2001). Variations between bands are rare, and restricted to occasional samples with lower total SiO_2 contents. The syn-kinematic (Alpine) mineral assemblage of the gneiss, characteristic of the peak of metamorphism, is garnet + biotite + muscovite + quartz + plagioclase ± paragonite. Accessory phases include ilmenite, monazite and tourmaline. The presence of paragonite is restricted to layers with lower SiO_2 contents. Complexly zoned garnet grains have only been found in the paragonite-bearing rocks.

The zoned garnet grains are small (1–3 mm), euhedral and undeformed, only rarely display evidence of retrogression to chlorite at their rims and are distributed evenly throughout hand-specimen sized examples of the gneiss. Electron microprobe analyses and X-ray maps of the garnet grains reveal complex almandine-grossular zonation (Fig. 1; Table 1). Garnet is the only phase in the sample to exhibit chemical zonation.

Prior to Alpine metamorphism, the present regional context of the sample allows one to presume that this paragneiss was influenced not only by magmatism at 1 Ga, but also magmatism during the Cambrian (at 475 ± 81 Ma, Stille and Tatsumoto, 1985) and by metamorphism during the Variscan orogeny (Von Raumer, 1998). Despite such a long polymetamorphic history there are no mineral relics observed in the assemblage, and garnet porphyroblasts contain only a few inclusions of quartz and, more rarely, allanite. No geochronological data are available and there is no petrographic evidence to suggest that the studied garnet grains represent zones that grew in different events. In the absence of more orthodox evidence, such as relics and inclusions in prophyroblasts, the reactions occurring on the prograde path of the studied rock and its P–T path are difficult, if not impossible, to define.

An approach based on the bulk rock composition of the sample has been investigated. With the DOMINO software (de Capitani and Brown, 1987; de Capitani, 1994; Biino and de Capitani, 1995), an internally consistent thermodynamic database and bulk rock compositions, we have calculated P–T equilibrium phase diagrams. Isopleths for almandine, grossular, Ca in plagioclase and Fe in epidote-clinozoite are calculated to predict how the equilibrium composition of each phase changes in response to variations in pressure and temperature. The modelled reactions and chemical changes are then compared to the observed zoning preserved in garnet.

The aim of this paper is: (1) to describe the methodology used in this study; (2) to apply the method to zoned garnet grain bearing garnet–biotite–muscovite gneiss from the Berisal Complex; and, (3) to discuss the potential and limitations of the method with respect to understanding metamorphic and geodynamic processes occurring in metamorphic terranes.

2. Methodology

We will illustrate the relationship between P and T of equilibration and observed chemical zoning in garnet and highlight the role of the different mineral reactions occurring in the rock during its metamorphic evolution. We approach this problem by correlating calculated equilibrium phase diagrams and mineral chemical isopleths with petrographical and chemical observations.

The limits of each stable equilibrium mineral assemblage in the phase diagram are indicated by lines. Each line represents a chemical reaction where one mineral assemblage breaks down and a new assemblage is stable. Isopleths join points of identical mineral composition in a phase diagram.

2.1. Electron Microprobe Analytical Procedures

Electron probe microanalysis of minerals was made using the JEOL JXA-8600 electron microprobe at the University of Basel operating in the wavelength dispersive mode. The microprobe is equipped with 4 crystal spectrometers and Voyager software by Noran Instruments. Individual spot analyses were made using a focussed electron beam with a beam diameter of 2 μm. The accelerating voltage was 15 kV, the beam-current was 10 nA and counting times were between 10 and 20 seconds. A combination of well characterised natural and synthetic standards was used for calibration, and a PROZA-type correction procedure was used for all data reduction.

X-ray maps showing the 2-dimensional distribution of selected major elements were produced on the same electron microprobe (using the energy dispersive system). Beam currents of 40 nA were used at 15 kV, with a dwell time of 0.2 seconds per pixel. Trace element distribution was mapped using the Cameca SX-100 electron microprobe at the University of Oslo, operating in WDS mode with 5 crystal spectrometers. Accelerating voltages of 20 kV, beam currents of up to 500 nA, and dwell times of up to 2.5 seconds per pixel were employed.

Table 2 XRF derived and modified bulk rock compositions for garnet–biotite–muscovite gneiss.

Bulk composition	1	1	2	3
Species	XRF Analysis (oxides, wt.%)	Bulk Composition[a] (At. Proportions)	Modified Composition 1[b] (At. Proportions)	Modified Composition 2[c] (At. Proportions)
Si	55.48	54.83	58.49	62.76
Al	20.50	23.88	21.60	23.13
Fe	9.81	8.11	9.43	4.36
Mn	0.21	0.18	0.04	0.01
Mg	2.59	3.82	2.69	2.51
Ca	1.74	1.84	1.61	0.88
Na	1.03	1.97	1.09	1.17
K	3.85	4.85	4.06	4.37
Ti	0.95	0.71	1.00	1.08
P	0.89	-	-	-
O	-	164.06	167.73	172.91
L.O.I.	2.34	-	-	-
Total	99.39	-	-	-

Notes: (a) Initial bulk rock composition input for calculation shown in Fig. 2a. (b) Bulk rock composition modified by subtracting the volume-composition of garnet cores (zone 1) from initial XRF derived bulk rock composition. (c) Bulk rock composition input for calculation shown in Fig. 3 calculated by subtracting the volume-composition of garnet zones 1 and 2 from initial XRF derived bulk rock composition.

2.2. Bulk Compositions

The bulk rock composition of the sample chosen for investigation was obtained by X-ray fluorescence spectroscopy (XRF) (Table 2). A sample of garnet–biotite–muscovite gneiss measuring approximately 15 × 10 × 12 cm and weighing ~5.5 kg was selected for chemical analysis (Volborth, 1969). The sample was sliced at regular intervals to check for abnormally large garnet porphyroblasts (>5 mm) and quartz ± feldspar concretions (>1 cm) that may skew chemical analysis. The slabs were passed through a jaw crusher, rendering 1–2 cm fragments, which were reduced to fine powder chemically representative of the bulk rock, in a tungsten-carbide disc mill.

Major oxide concentrations (Table 2) were determined on glass beads, with a diameter of 20 mm, prepared using 300 mg of crushed rock powder and 4700 mg of lithium tetraborate. Analysis was made on a Siemens SRS3000 wavelength dispersive X-ray spectrometer with a Rh end window tube (4 kV). Results were collected and evaluated using the Bruker AXS Spectraplus standardless evaluation programme.

The strong and complex chemical zoning in the garnet grains implies chemical fractionation of the bulk rock composition, and evidence that the rock did not completely equilibrate during metamorphism. To evaluate the influence of the zoned garnet grains on effective bulk-composition, the percentage volume of garnet in the rock and the partial volume of each chemical zone were calculated by digital image analysis of whole thin sections and X-ray maps of representative garnet grains. The effective composition of each chemical zone in garnet was then subtracted from the original bulk rock composition (Table 2).

2.3. Thermodynamic Modelling

Thermodynamic analysis is based on equilibrium phase diagrams for the $Na_2O–CaO–K_2O–FeO–MgO–Al_2O_3–SiO_2–H_2O$ system calculated with the thermodynamic software DOMINO (e.g. de Capitani, 1994). This approach computes equilibria by minimisation of the total Gibbs free energy for a fixed composition over a defined range of P and T. The initial input for the calculation was the bulk rock chemistry obtained via XRF analysis, and converted to atomic percent (Table 2). We used the updated thermodynamic database JUNE.92 of Berman (1988) to calculate equilibrium phase assemblages. The database was supplemented with internally consistent additions for omphacite (Meyre et al., 1997), phengite (Massonne and Szpurka, 1997), Mg-glaucophane (Evans, 1990), Fe-glaucophane and daphnite (Le Bayon, 2002), and solution models for phengite (Massonne and Szpurka, 1997), feldspar (Fuhrman and Lindsley, 1988), garnet (Berman, 1990), and staurolite (Nagel, 2002). Ideal Fe–Mg mixing on site is assumed for biotite ($a_{Ann}=(X_{Fe}^M)^3$, $a_{Phl}=(X_{Mg}^M)^3$), clinozoisite-epidote ($a_{Czo}=(X_{Al}^M)$,

$a_{Ep}=(X_{Fe}{}^M))$, chlorite $(a_{Dap}=(X_{Fe}{}^M)^5$, $a_{Cln}=(X_{Mg}{}^M)^5)$, cordierite $(a_{Fe-Crd}=(X_{Fe}{}^M)^2$, $a_{Mg-Crd}=(X_{Mg}{}^M)^2)$ and glaucophane $(a_{Fe-Gln}=(X_{Fe}{}^M)^3$, $a_{Mg-Gln}=(X_{Mg}{}^M)^3)$ with Cln = clinochlore, Dap = daphnite, and all other abbreviations after Kretz (1983).

SiO$_2$ and H$_2$O are assumed to be in excess in our calculations. Absolute uncertainty in the position of individual boundaries between phase assemblages, propagated from uncertainty in the thermodynamic data used for compilation of the database and solid solution models, is ± 2 kbar and ± 30 °C.

3. Application of the Method

3.1. Garnet Zoning and Mineral Chemistry

Chemical profiles of garnet (Fig. 1B) show Mn-rich cores and classic bell-shaped spessartine profiles indicating that they grew on the prograde metamorphic path. The pyrope profile is inversely related to the spessartine profile, and has an up-turned bell-shape (Fig. 1B). Similarly, the almandine and grossular contents are inversely related to each other. However the chemical profiles in these elements are more complex (Fig. 1). Moving from the centre of each crystal (Fig. 1; zone 1), the X_{Grs} profile shows a sharp increase to a plateau (Fig. 1; zone 2), thereafter a sharp decrease and a plateau (Fig. 1, zone 3). In some grains a sharp enrichment of Ca is observed near the rim (Fig. 1; point 4). The X_{Alm} values mirror the X_{Grs} profile, with a sharp decrease after crystallisation and then a gradual increase. This is followed by a sharp increase and a second zone of gradually increasing X_{Grs}. Close to the rims, correlated with the X_{Grs} "spike", a sharp decrease in X_{Alm} is observed. The nearby mica minerals are all chemically homogenous, while plagioclase is of oligoclase composition (Ab$_{75}$)(Fig. 1; Table 3).

Trace element maps of P, Y, Cr and Zn were collected, but the concentrations are very low and do not show any heterogeneity across garnet grains. The Ti map is more complex with enrichment at the core.

3.2. Interpretation of Complex Chemical Zonations in Garnet Through Modelling

Figure 2 shows P–T equilibrium phase diagrams, with mineral isopleths for grossular, almandine, plagioclase and epidote, calculated for the original bulk rock composition of the garnet–biotite–muscovite gneiss (Table 2).

Table 3 Electron-microprobe analysis of mica species and plagioclase co-existing with garnet grains in garnet–biotite–muscovite gneiss.

	Paragonite		Muscovite		Biotite		Plagioclase	
SiO$_2$	47.6	46.9	47.9	47.4	36.9	36.8	59.8	61.0
TiO$_2$	0.11	<0.16	0.11	0.33	1.18	1.36	<0.16	<0.16
Al$_2$O$_3$	40.5	40.8	36.1	34.4	19.2	18.53	24.8	23.7
FeO	0.57	0.36	1.28	1.61	19.7	21.35	(n.a.)	(n.a.)
MnO	<0.02	<0.02	<0.02	<0.02	<0.02	<0.02	(n.a.)	(n.a.)
MgO	0.09	0.09	1.11	1.32	11.03	9.53	(n.a.)	(n.a.)
CaO	0.10	0.09	0.05	0.01	0.03	<0.02	6.36	5.45
BaO	<0.30	>0.30	0.13	0.19	<0.30	0.08	<0.30	<0.30
Na$_2$O	7.15	7.43	1.62	1.31	0.2	0.26	8.01	8.73
K$_2$O	0.81	0.81	9.44	9.65	8.97	9.21	0.11	0.09
Total	96.98	96.24	97.66	96.21	97.15	97.09	99.06	98.97
Si	5.98	5.92	6.19	6.25	5.47	5.52	2.69	2.74
Ti	0.01	0.00	0.01	0.03	0.13	0.15	0.00	0.00
Al	6.01	6.08	5.50	5.33	3.35	3.28	1.31	1.25
Fe	0.06	0.04	0.14	0.18	2.45	2.68	-	-
Mn	0.00	0.00	0.00	0.00	0.00	0.00	-	-
Mg	0.02	0.02	0.21	0.26	2.44	2.13	-	-
Ca	0.01	0.01	0.01	0.00	0.00	0.00	0.31	0.26
Ba	0.00	0.00	0.01	0.01	0.00	0.00	0.00	0.00
Na	1.74	1.82	0.41	0.33	0.06	0.08	0.70	0.76
K	0.13	0.13	1.56	1.62	1.70	1.76	0.01	0.01
Total	13.95	14.02	14.08	14.03	15.60	15.61	5.01	5.02

n.a. — not analysed.
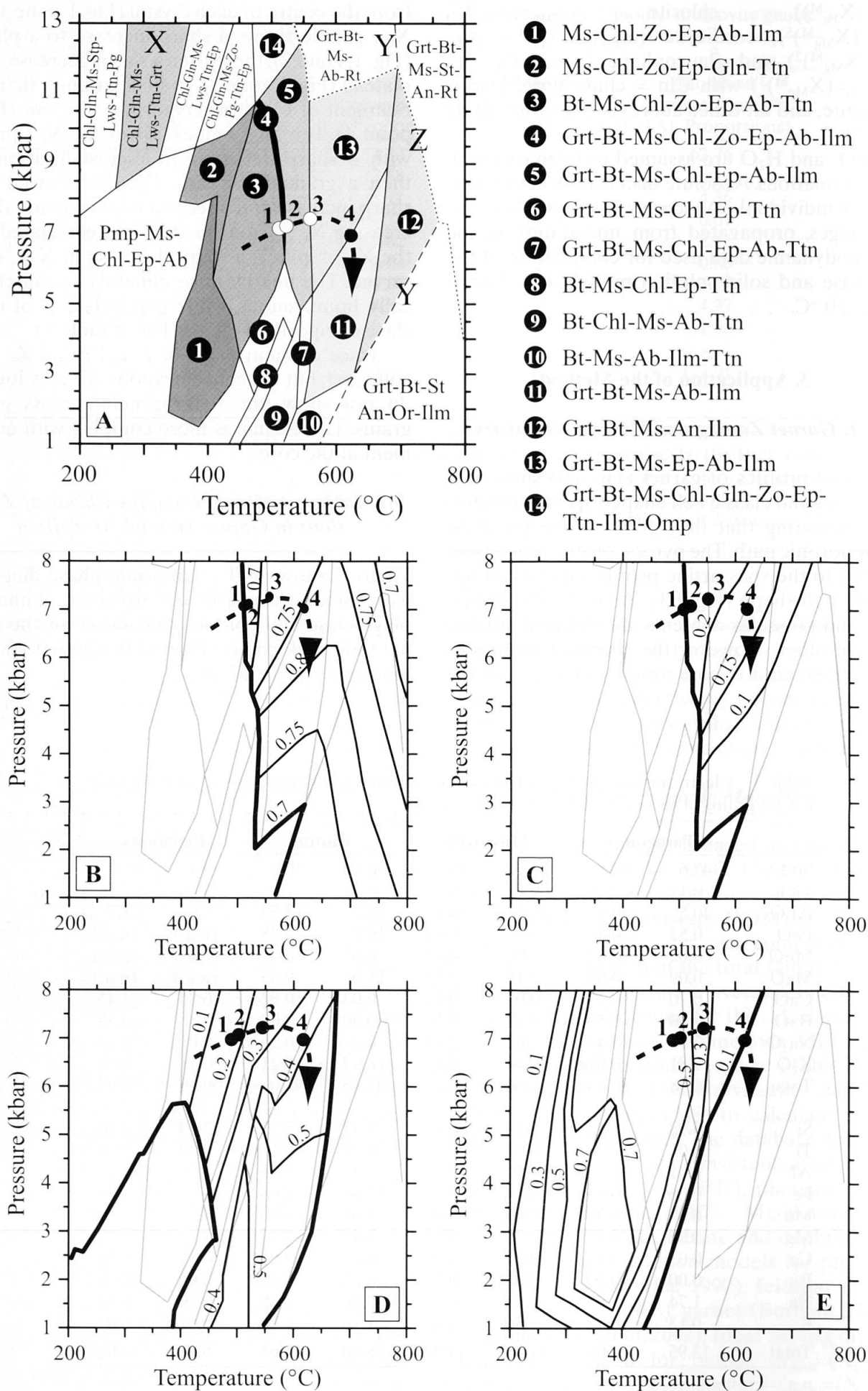
Fig. 2

Table 4 Overview of important calculated mineral assemblages.

Zone	T (°C)	Calculated Assemblage
Pre-garnet formation	<500	Bt+Ms+Chl+Zo+Ep+Ab+Ttn+Qtz+H$_2$O
Core – 1	500	Grt+Bt+Ms+Chl+Ep+Ab+Ilm+Qtz+H$_2$O
2	>520 <560	Grt+Ms+Bt+Ep+Ab+Ilm+Qtz+H$_2$O
3	>570 <670	Grt +Ms+Bt+Ab+Ilm+Qtz+H$_2$O

Several observations can be made that set limits on the shape and trajectory of the reconstructed prograde P–T path. There are two regions in P–T space (Fig. 2a) where garnet is stable but the observed and calculated garnet compositions indicate a path that only passes through the higher temperature field. The calculated composition for the high-pressure, lower-temperature garnet is grossular-rich (X_{Gr} = 0.8) (Area X; Fig. 2A) while the observed garnet cores are grossular-poor and almandine-rich, more similar to those of the calculated higher-temperature garnet field (Figs 2B–C). Therefore, the first nucleation of garnet on the prograde P–T path is defined by a point at the intersection between the plotted path and the higher temperature garnet stability field (point 1, Fig. 2A). The dashed reaction line, Y, is the staurolite-in isograd (Fig. 2A). There is no staurolite in the rocks and we surmise that the P–T path did not enter the staurolite field. The dotted reaction line Z (Fig. 2A) is the transition of ilmenite to rutile towards higher pressure and temperature. No rutile has been found anywhere in the sample, hence this reaction provides an upper pressure limit for the P–T path.

Between the garnet-in line at Point 1 (Fig. 2B) and the staurolite-in reaction, three metamorphic reactions and one phase change were calculated to occur with increasing T; each may be used to interpret the observed chemical zoning in garnet. The low-Ca garnet cores nucleated and grew, with increasing temperature, from a Bt–Ms–Chl–Zo–Ep–Ab–Ttn–Qtz–H$_2$O assemblage (Figs. 2A, Pt. 1). The nucleation of garnet is concomitant with the breakdown of titanite and the formation of ilmenite. Following garnet nucleation, the increase

in X_{Grs} content (Fig. 1) indicates the breakdown of a Ca-phase. This change in garnet chemistry is reflected in the zoisite-out line at immediately higher temperatures, stabilizing Ca-richer garnet and more calcic-plagioclase (Figs. 2A, 2C; Pt. 2). Along a continuous prograde path two further reactions are predicted: (1) Chlorite becomes thermodynamically unstable and is replaced by Fe-rich garnet. During chlorite breakdown (Fig. 2B; Pt. 3) Fe and Mg are released, and X_{Alm} and X_{Prp} increase (Figs. 1B, 2B). We interpret from our modelling that this garnet grew in equilibrium with a Bt–Ms–Ep–Ab–Ilm–Qtz–H$_2$O assemblage; and (2) epidote stability continuously decreases in favour of clinozoisite, releasing Fe into the local chemical system promoting Fe-richer garnet (Figs. 1, 2B, 2E) in a Gt–Bt–Ms–Ep–Ab–Ilm–Qtz–H$_2$O assemblage.

The epidote-out reaction (Fig. 2A; Pt. 4) results in further fractionation of Fe into garnet (Figs. 1, 2B) and Ca into plagioclase (Fig. 2D). The calculated equilibrium assemblage (Gt–Bt–Ms–Ab–Ilm–Qtz–H$_2$O) reflects the observed peak metamorphic assemblage in the rock. Whilst the staurolite-in reaction occurs at higher temperatures, providing the only positive control on peak temperature, the high Na/Ca ratio of plagioclase (Table 3) in the assemblage suggests that the Gt–Bt–Ms–Ab–Ilm–Qtz–H$_2$O assemblage is characteristic of the peak assemblage, i.e. assemblage 12 (Fig. 2A; Gt–Bt–Ms–An–Ilm–Qtz–H$_2$O) was not reached by the P–T path.

The sequence of mineral formation and breakdown reactions resulting from the evolving P–T conditions has been established (Table 4), and a maximum pressure of nearly 7.5 kbar and maxi-

Fig. 2 Calculated equilibrium phase diagrams for the zoned garnet-grain-bearing garnet–biotite–muscovite gneiss. White numbers in black circles refer to stable assemblage fields. Black numbers and associated points refer to reactions discussed in the text. (A) P–T equilibrium phase diagram calculated for the bulk composition 1 (derived from XRF analysis; Table 2) with SiO$_2$ and H$_2$O in excess. (B) Almandine isopleths calculated for bulk rock composition 1 (Table 2). (C) Grossular isopleths calculated for bulk rock composition 1 (Table 2). (D) Anorthite content in plagioclase isopleths calculated for bulk rock composition 1 (Table 2). (E) X_{Fe} isopleths in epidote calculated for bulk rock composition 1 (Table 2).

① Ms-Chl-Ep-An-Ttn
② Bt-Ms-Chl-Ep-Ab-Ttn-Omp
③ Bt-Ms-Chl-Ep-Ab
④ Grt-Bt-Ms-Chl-Ep-Ab-Ilm
⑤ Grt-Bt-Ms-Ab-Ttn-Ilm
⑥ Bt-Ms-Chl-Ab-Ilm
⑦ Grt-Bt-Ms-Chl-Ab-Ilm
⑧ Gt-Bt-Ms-Ab-Ilm-Crd
⑨ Grt-Bt-Ms-Ab-Ilm
⑩ Grt-Bt-Ms-An-Ilm
⑪ Grt-Bt-An-Rt-Sil
⑫ Grt-Bt-Ms-Ep-Ab-Ilm
⑬ Grt-Bt-Ms-Ab-Ttn-Ilm
⑭ Grt-Bt-Ms-Ab-Ttn-Ilm-Rt
⑮ Grt-Bt-Ms-Ab-Ilm-Rt
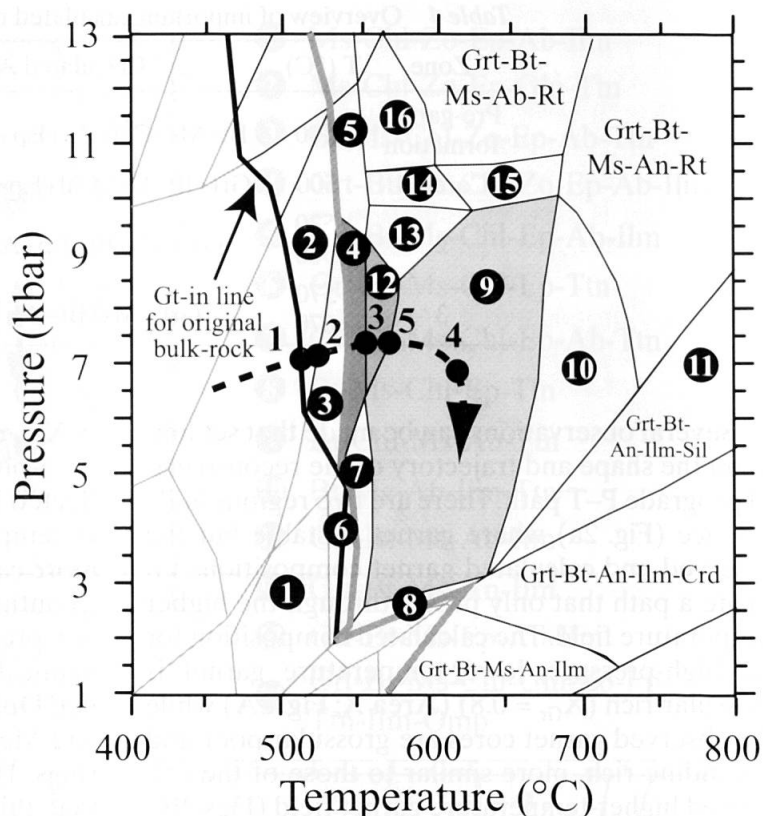⑯ Grt-Bt-Ms-Ab-Ttn-Rt

Fig. 3 Calculated equilibrium phase diagram for modified bulk rock composition 3 (Table 2). White numbers in black circles refer to stable assemblage fields. Black numbers and associated points refer to reactions discussed in the text.

mum temperature of 650 °C has been deduced for the Alpine metamorphism of the Berisal Complex. The conditions are in good agreement with all previous work on the metamorphism of the area (Stille, 1980; Stille and Tatsumoto, 1985; Todd and Engi, 1997).

3.3. The Ca-Spike at the Garnet rim

The peak of metamorphism in the phase diagram (Fig. 2) lies between the epidote-out and the staurolite-in reactions. Between these two reactions there are no other mineral-forming (or mineral breakdown) reactions. Plagioclase compositions do change continually, from sodic to intermediate, but there are no calculated reactions to provide a suitable explanation for the Ca-spike near the edge of the garnet grains.

The garnet compositions either side of the Ca-spike are similar (Fig. 1). The breadth of the Ca-spike fluctuates between 5 and 25 μm, and at some points is seen to be almost absent. We infer a transient change in the local chemical composition to account for the Ca-spike, probably due to the breakdown of a Ca-bearing accessory phase.

Common Ca-bearing accessory phases in metapelites include apatite, titanite, and allanite. No

apatite remains in the rock, and X-ray maps display no increase in phosphorus close to the garnet rim, hence it is difficult to evaluate the influence of apatite during metamorphism. Titanite is found in the calculated P–T diagram, but reacted out during garnet nucleation (Fig. 2, Pt. 1), hence its breakdown cannot be invoked to explain the Ca-spike. On the other hand, Smith and Barreiro (1990) suggested that allanite breaks down to form monazite during prograde metamorphism at temperatures above 525 °C, whilst Wing et al. (2003) provided evidence for the reaction occurring around 550 °C. Allanite has not been found in the matrix of the garnet–biotite–muscovite gneiss, but is found as inclusions in some garnet grains. One possible explanation for the Ca-spike could be the prograde breakdown of matrix allanite to monazite. Its Ca was concentrated in the garnet resulting in the observed spike while the rare earth elements were taken up by monazite.

3.4. Influence of Bulk Rock Chemical Fractionation

Isochemical P–T phase diagrams were calculated with each modified composition (Table 2) and compared with the original; the calculated phase

diagram is presented for the bulk rock composition minus garnet zones 1 and 2 (Fig. 3). This is intended to represent the phase relations in the rock close to the peak of metamorphism for what is calculated to be the effective bulk rock composition after early prograde garnet growth.

For this modified bulk composition, the calculated assemblages along the derived P–T path in the phase diagram (Fig. 3), at temperatures above which garnet is stable, are the same as those calculated for the original bulk composition. The chlorite-out reaction, thought to be responsible for garnet zone 2, occurs at the same temperature for both bulk compositions (~560 °C at 7.4 kbar). The maximum pressure in Fig. 3 is lower; the rutile-in line being located just below 10 kbar compared to 11 kbar in Fig. 2A. The absence of rutile can also be used to constrain T_{max} between 675 and 730 °C for pressures >6.5 kbar, while the absence of sillimanite in the observed assemblage limits it to the same temperature range <6.5 kbar (Fig. 3). However, as in Fig. 2, the presence of sodic rather than intermediate plagioclase in the observed assemblage, supports a peak temperature of <650 °C.

The most significant contrast between the two calculations is the lower temperature for the epidote-out reaction (Fig. 3, Pt. 5, compared to Fig. 2, Pt. 4). It is calculated to occur at 570 °C for the modified bulk rock composition 3 (Table 2), rather than ~620 °C, for the original bulk rock composition derived via XRF. This minimum temperature is higher than that proposed for the breakdown of allanite in regionally metamorphosed paragneiss, and the proposed explanation for the Ca-spike is valid.

4. Discussion

The calculation of isochemical P–T phase diagrams in metamorphic petrology and their interpretation to aid understanding of the growth of metamorphic minerals and/or assemblages, the development of metamorphic domains, or chemical zonation in minerals has become increasingly popular in recent years (e.g. Brouwer and Engi, 2005; Tinkham and Ghent, 2005; Zeh, 2001a; Zeh, 2001b; Tóth et al., 2000). However, the success of the technique is dependent on appreciating its limitations and inherent uncertainties

In this study the first set of limitations that must be considered concern uncertainty in the thermodynamic database propagated from experimental error. Furthermore, the reliability of the thermodynamic data for some minerals is particularly poor; for example there are no reliable experimental results for daphnite and Fe-glaucophane, and their data was optimised by theoretical methods (Le Bayon, 2002). Furthermore, the simplification of the solid solution model for chlorite, clinozoisite-epidote, cordierite and glaucophane may also affect calculations. This paper presents equilibrium phase diagrams for the garnet–biotite–muscovite gneiss calculated in the CaNKFMASH system; we do not integrate phosphate or rare earth element minerals in our model (e.g. apatite, monazite or allanite), which may affect mineral assemblage stability, because of the lack of thermodynamic data and experimental calibrations. Nor do we include MnO, which may also influence mineral stability, particularly garnet, a mineral which is more stable at lower temperatures when Mn is present (Symmes and Ferry, 1992).

A more significant source of error, which is not systematic and should be addressed in all calculations for an isochemical system, is the uncertainty in the effective bulk rock composition of the equilibration volume. Errors in the effective bulk rock composition used in the calculations may be introduced during sample collection and chemical analysis (small samples with large and numerous porphyroblasts may skew analysis), by failure to account for fractionation of the bulk rock composition due to porphyroblast growth (Marmo et al., 2002) (a problem that may be exacerbated if the porphyroblats are chemically zoned), and the effects of adding or removing chemical components by the action of fluid and/or partial melting, while preserving an earlier assemblage (White and Powell, 2002).

For the sample of garnet–biotite–muscovite gneiss described, any uncertainty between the bulk rock composition obtained via XRF analysis and that of effective reaction volume was minimised by analysing a petrographically representative sample sufficiently large to eradicate the influence of porphyroblasts measuring ≥1 cm (of which none >5 mm were found during sample preparation), and with no domain development. Furthermore, the influence of chemical fractionation, as documented in the zoned garnet grains was evaluated. While no evidence for partial melting has been documented anywhere in the Berisal Complex, late-Alpine quartz veining has influenced bulk rock SiO_2 concentrations at some localities (Hetherington et al., 2003). However the effect is restricted to within 50 cm of a vein; no quartz veins were observed within 10 m of the present sampling point.

The calculated assemblages for the predicted P–T path in the phase diagram for the modified bulk rock composition, at temperatures above which garnet is stable, are the same as those calculated for the original bulk rock composition. Sim-

ilarly, the chlorite-out reaction, responsible for the development of garnet zone 2, occurs at the same temperature for both bulk rock compositions (~560 °C at 7.4 kbar). However, the P–T conditions at which the assemblages, calculated with the modified bulk rock composition, did change with respect to the original calculation showing that the influence of effective bulk-composition should be addressed. In this case, the results allow us to place tighter constraint of the peak metamorphic conditions: The upper pressure limit with the rutile-in line is slightly below 10 kbar, compared to 11 kbar in Fig. 2. The absence of rutile and sillimanite in the observed assemblage constrains T_{max} to between 675 and 730 °C for pressures over and below 6.5 kbar respectively. However, albitic plagioclase in the observed assemblage requires $T_{max} < 650$ °C. The lower temperature limit, marked by the epidote-out reaction, occurs at 570 °C rather than ~620 °C for the modified bulk composition. This decreases the lower temperature limit for peak metamorphism.

5. Conclusions

Garnet grains in a garnet–biotite–muscovite paragneiss from the Berisal Complex (Simplon Region) show complex chemical zonation. Apart from the Alpine mineral assemblage observed, the rock contains no petrographic indicators, such as mineral relics of poikiloblasts, that aid interpretation of the rock's metamorphic history.

Thermodynamic modelling of the rock, using bulk rock chemistry and the DOMINO software indicates that three net transfer reactions occurred between garnet nucleation and the peak of metamorphism. The inferred influence of these reactions on the local composition has been used to explain the chemical zonation observed in garnet.

The influence of garnet porphyroblast growth on the effective bulk-composition has been evaluated. Although there is no change in the order and nature of the net transfer reactions during porphyroblast growth, the P–T conditions of some reactions changed: The minimum estimate for T_{max} in the Berisal Complex could be as low as 570 °C.

References

Berman, R.G. (1988): Internally-consistent thermodynamic data for mineral in the sytem Na_2O-K_2O-CaO-MgO-FeO-Fe_2O_3-Al_2O_3-SiO_2-TiO_2-CO_2. *J. Petrol.* **29**, 445–522.

Berman, R.G. (1990): Mixing properties of Ca–Mg–Fe–Mn garnets. *Am. Mineral.* **75**, 328–344.

Biino, G.G. and de Capitani, C. (1995): Equilibrium assemblage calculations; a new approach to metamorphic petrology. In: *Studies on metamorphic rocks and minerals of the Western Alps; a volume in memory of Ugo Pognante (1954–1992)* (ed Lombardo, B.) *Bollettino – Museo Regionale di Scienze Naturali.* pp. 11–53, Museo Regionale di Scienze Naturali, Torino.

Brouwer, F.M. and Engi, M. (2005): Staurolite and other aluminous phases in Alpine ecolgite from the Central Swiss Alps: Analysis of domain evolution. *Can. Mineral.* **43**, 105–128.

Chernoff, C.B. and Carlson, W.D. (1997): Disequilibrium for Ca during growth of pelitic garnet. *J. Metamorphic Geol.* **15**, 421–438.

de Capitani, C. (1994): Gleichgewichts-Phasendiagramme: Theorie und Software. *Beiheft z. Deutschen Mineral. Gesellschaft* **6**, 1–48.

de Capitani, C. and Brown, T. H. (1987): The computation of chemical equilibrium in complex systems containing non-ideal solutions. *Geochim. Cosmochim. Acta* **51**, 2639–2652.

Escuder Vituete, J., Indares, A. and Arenas, R. (2000): P–T paths derived from garnet growth zoning in an extensional setting: an example from the Tormes Gneiss Dome (Iberian Massif, Spain). *J. Petrol.* **41**, 1489–1515.

Evans, B.W. (1990): Phase relations of epidote-blueschists. *Lithos.* **25**, 3–23.

Fuhrman, M.L. and Lindsley, D.H. (1988): Ternary feldspar modeling and thermometry. *Am. Mineral.* **73**, 201–215.

Hetherington, C.J. (2001): Barium anomalies in the Berisal Complex, Simplon Region, Switzerland. *Unpub. Ph.D. Thesis, Universität Basel, Basel.*

Hetherington, C.J., Mullis, J., Graeser, S. and Gieré, R. (2003): The formation of armenite in the Berisal Complex, Simplon Region, Switzerland. *Schweiz. Mineral. Petrogr Mitt.* **83**, 243–259.

Kreissig, K., Holzer, L., Frei, R., Villa, I.M., Kramers, J.D., Kröner, A., Smit, C.A. and van Reene, D.D. (2001): Geochronology of the Hout River Shear Zone and the metamorphism in the Southern Marginal Zone of the Limpopo Belt, Southern Africa. *Precambr. Res.* **109**, 145–173.

Kretz, R. (1983): Symbols for rock-forming minerals. *Am. Mineral.* **68**, 277–279.

Le Bayon, R. (2002): Tectono-Metamorphic Evolution of the Monte Rosa Nappe and Surrounding units (Western Alps): Implications for Alpine Geodynamics and exhumation of Metamorphic Terranes. *Unpub. Ph.D. Thesis, University of Basel, Basel.*

Marmo, B.A., Clarke, G.L. and Powell, R. (2002): Fractionation of bulk rock composition due to porphyroblast growth: effects on eclogite facies mineral equilibria, Pam Peninsula, New Caledonia. *J. Metamorphic Geol.* **20**, 151–165.

Massonne, H.-J. and Szpurka, Z. (1997): Thermodynamic properties of white micas on the basis of high-pressure experiments in the systems K_2O-MgO-Al_2O_3-SiO_2-H_2O and K_2O-FeO-Al_2O_3-SiO_2-H_2O. *Lithos* **41**, 229–250.

Meyre, C., de Capitani, C. and Partzsch, J.H. (1997): A ternary solid solution model for omphacite and its application to geothermobarometry of eclogites

from the Middle Adula nappe (Central Alps, Switzerland). *J. Metamorphic Geol.* **15**, 687–700.

Nagel, T. (2002): Metamorphic and structural history of the Southern Adula Nappe (Graubünden, Switzerland). *Unpub. Ph.D. Thesis, University of Basel, Basel.*

O'Brien, P.J. (1999): Asymmetric zoning profiles in garnet from HP–HT granulite and implications for volume and grain-boundary diffusion. *Mineral. Mag.* **63**(2), 227–238.

O'Brien, P.J. and Vrana, S. (1997): Eclogites with a short-lived granulite facies overprint in the Moldanubian Zone, Czech Republic: petrology, geochemistry and diffusion modelling of garnet zoning. *Geol. Rundsch.* **84**, 473–488.

Rollinson, H. (2003): Metamorphic history suggested by garnet-growth chronologies in the Isua Greenstone Belt, West Greenland. *Precambr. Res.* **126**, 181–196.

Simon, G., Chopin, C., and Schenk, V. (1997): Near-end-member magnesiochloritoid in prograde-zoned pyrope, Dora-Mairia massif, western Alps. *Lithos* **41**, 37–57.

Smith, H.S. and Barreiro, B. (1990): Monazite U–Pb dating of staurolite grade metamophism in pelitic schists. *Contrib. Mineral. Petrol.* **105**, 602–615.

Stille, P. (1980): On the genesis of the amphibolites and hornblendfelses in the Berisal Complex (Simplon; Italy–Switzerland). *Mem. Ist. Geol. Padova.* 34, 205–246

Stille, P. and Tatsumoto, M. (1985): Precambrian tholeiitic-dacite rock-suites and Cambrian ultramafic rocks in the Pennine napped system of the Alps: Evidence from Sm–Nd isotopes and rare earth elements. *Contrib. Mineral. Petrol.* **89**, 184–192.

Stuewe, K. (1997): Effective bulk composition changes due to cooling: a model predicting complexities in retrograde reaction textures. *Contrib. Mineral. Petrol.* **129**, 43–52.

Symmes, G.H. and Ferry, J.M. (1992): The effect of whole-rock MnO content on the stability of garnet in pelitic schists during metamorphism. *J. Metamorphic Geol.* **10**, 221–237.

Tinkham, D.K. and Ghent, E.D. (2005): Estimating P–T conditions of garnet growth with isochemical phase-diagram sections and the problem of effective bulk-composition. *Can. Mineral.* **43**, 35–50.

Todd, C.S. and Engi, M. (1997): Metamorphic field gradients in the Central Alps. *J. Metamorphic Geol.* **15**, 513–530.

Tóth, T.M., Grandjean, V. and Engi, M. (2000): Polyphase evolution and reaction sequence of compositional domains in metabasalt: a model based on local chemical equilibrium and metamorphic differentiation. *Geol. J.* **35**, 163–183.

Volborth, A. (1969): *Elemental Analysis in Gechemistry.* Elsevier.

Von Raumer, J.F. (1998): The Palaeozoic evolution in the Alps: from Gondwana to Pangea. *Geologische Rundsch.*, **87**, 407–435.

White, R.W. and Powell, R. (2002): Melt loss and the preservation of granulite facies mineral assemblages. *J. Metamorphic Geol.* **20**, 621–623.

Wing, B.A., Ferry, J.M. and Harrison, T.M. (2003): Prograde destruction and formation of monazite and allanite during contact and regional metamorphism of pelites: petrology and geochronology. *Contrib. Mineral. Petrol.* **145**, 228–250.

Zeh, A. (2001a): Inference of a detailed P–T path from P–T pseudosections using metapelitic rocks of variable composition from a single outcrop, Shackleton Range, Antarctica. *J. Metamorphic Geol.* **19**, 329–350.

Zeh, A. (2001b): Reconstruction of prograde P–T paths from zoned garnet and mineral inclusions using phase diagrams, problems and solutions. In: *EUG XI J. Conf. Abs.* pp. 869, Cambridge Publications, Strasbourg.

Zeh, A. and Holness, M.B. (2003): The effect of reaction overstep on garnet microtextures in metapelitic rocks of the Ilesha Schist Belt, SW Nigeria. *J. Petrol.* **44**, 967–994.